FREQUENCY RESPONSE OF ACTIVE DIPOLE Antennas

A Thesis

Presented to

The Faculty of Graduate Studies and Research

The University of Manitoba

In Partial Fulfillment

of the Requirements for the Degree

Master of Science in Electrical Engineering

by

Isao Furukawa

July 1971

ABSTRACT

The thesis presents a technique for improving the bandwidth and the receiving gain of a passive dipole antenna by introducing a special transistor circuit at the feed point. The circuit utilizes the inductive property of a transistor amplifier, thus providing a good impedance match over an appreciable portion of the frequency range in which the dipole is capacitive. The base resistor of this amplifier has a significant effect on the gain and the bandwidth, and lowers the center frequency at which the gain is maximum. It is shown that the improvement in gain, due to this circuit, of a 44.8 cm long dipole operating at 220 MHz is 9 dB while the VSWR becomes 1.54 as compared to 29.6 for the passive antenna. It is also shown that, due to the noise temperature of the active circuit, there is a noise-limited frequency band for which the maximum net gain improvement is 10.6 dB at 290 MHz.

ACKNOWLEDGMENTS

The author expresses his sincere appreciation to Professors M.A.K. Hamid and M. Yunik who suggested the problem and took an active interest in the work throughout.

Thanks are due to friends and colleagues for their comments and discussions.

Financial support was provided in part by the National Research Council of Canada.

TO MY PARENTS

WITH DEEP GRATITUDE AND

AFFECTION

TABLE OF CONTENTS

LIST OF FIGURES

CHAPTER I

INTRODUCTION

The study of active antennas occupies a prominent position in antenna theory, particularly since many new types of high frequency semiconductors have been recently developed. An active antenna system is a combination of a passive antenna and a semiconductor circuit which may lead to higher gain or signal to noise ratio or, alternatively, a reduction in the overall length of the antenna for the same gain.

The current distribution of an active antenna is controlled by an active circuit when the circuit is connected to the passive antenna. The input impedance, the power gain, the beamwidth, and the field pattern are obviously influenced by the circuit configuration [1]. It should be noted that any advantages of an active antenna over a passive one are at the expense of complexity in the circuit as well as added interference, noise temperature and power dissipation.

The study of an active antenna has been facilitated ever since Hansen [2] reported special issue on active antennas. Some types of active antennas which have been developed and reported are the parametric amplifier antenna

[3,4], the Esaki diode antenna [5-9], and the transistorized antenna [10-12].

Frost [3,4] presented the parametric amplifier antenna using parametric diodes and a dipole antenna, and reported 23 dB maximum gain at 221 MHz relative to a passive dipole having the same length and diameter.

Fujimoto [5] presented a theoretical study of some properties of a tunnel-diode-loaded-dipole antenna and discussed gain, noise performance, stability, and reradiation characteristics. The analysis was performed by applying network theory techniques to an equivalent circuit of the active antenna. The author reported experiments of radiation patterns, maximum gain of 12 dB, and a few percent larger bandwidth of the tunnel-diode-loaded dipole antenna [6]. The author also reported the "antennafier" which is a dipole antenna combined with an Esaki diode circuit [7]. He employed a modified pi-match dipole to improve the overall performance of the antenna. The analysis of the "antennafier" was made by using an equivalent circuit derived by computing the impedance from radiating and nonradiating components of voltage and current. The gain, noise performance, and stability were discussed. Typical experimental results at a center frequency of 420 MHz showed that the bandwidth was several percent higher and the gain was 3 to 12 dB larger, while the noise figure was 5 to 6 dB higher at 420 MHz.

Copeland et al [9] reported "antennaverters" and "antennafiers" using a tunnel diode. The "antennaverter" is a passive antenna and a converter combined into a single unit, while the "antennafier" is a passive antenna and a r-f amplifier combined into a single unit. The authors discussed an analysis of the tunnel diode down converter and reported that the tunnel diode converter had a 14 dB gain with respect to the sensitivity of the standard dipole system with a coaxial mixer.

Copeland et al [10] reported a 12.5 dB higher gain relative to the reference dipole and a Q of 8.16 by using a common emitter transistorized dipole antenna operating between 135 and 165 MHz. The authors also described a four-element broadside array active antennas with a view of improving the half-power beamwidth, power gain and noise temperature over a half wave dipole.

Meinke [12] reported a transistor circuit mounted on a monopole antenna. He discussed the noise temperatures of the receiving system and the influence of bias on the impedance and radiation pattern between 800 kHz and 250 MHz. The author also examined various types of active antennas and showed that the resonance frequency could be shifted by changing the collector current of the second stage transistor circuit, whereas, the bandwidth could be varied by adjusting the collector current of the first stage transistor circuit. He reported that the VSWR of the active antenna was less than 2.5 in the frequency range of 2.5 to 25 MHz.

Recently many arguments have been brought forward regarding the noise of transistorized antennas. Meinke et al [13] reported that the noise temperature of the receiving transistorized antenna system was lower than that of the passive antenna. Landstorfer [14] reported a 10 dB gain of a transistorized antenna over a half wave dipole and showed that the noise temperature of a transistorized aerial system was smaller than that of a passive aerial. He reported that the minimum noise temperature of a particular active antenna configuration was 1470 K in the frequency range of 470 and 800 MHz.

The purpose of this thesis is to utilize the inductive impedance property of transistors, over a limited frequency range, in order to improve the gain and the bandwidth of a dipole antenna which is capacitive when the transistor is inductive. The active antenna, which is used as a receiving system, consists of two transistor stages and a passive dipole antenna. The first transistor stage is employed to get the inductive impedance property in order to improve the voltage gain and the bandwidth of the active dipole antenna. The inductive impedance property is utilized for obtaining a conjugate match between a passive antenna and the first stage (for maximum power transfer). The length of the passive antenna is chosen so that its impedance is capacitive.

The advantages of the active over the passive dipole antenna of the same geometrical dimensions are : higher gain, larger bandwidth, lower center frequency and lower noise temperature of the receiving system within a narrow frequency range.

In chapter II, the short circuit Y admittance parameters, the open circuit Z impedance parameters and the ABCD transmission parameters are used to describe the circuit configuration of the transistor amplifiers and the corresponding active antenna. The common base transistor circuit configuration and the noise temperature of the receiving system are also discussed. The theoretical frequency response of an active antenna is calculated using an IBM 360/OS model 65 digital computer and the results are reported in graphical form.

Experimental procedures for various parameters are discussed and the measured data are presented in chapter III. These consist of measuring the input admittance of the passive antenna , transistor Y parameters, input admittance of the transistor circuits, output admittance and relative gain of the active antenna.

The theoretical and experimental results are discussed along with suggestions for further research in chapter IV.

CHAPTER II

CIRCUIT CONFIGURATIONS

In this chapter the circuit configurations of active and passive antennas are presented. The theoretical characteristics of these antennas are compared with emphasis on frequency response and noise temperature.

2.1 Equivalent Circuit of Common Base Transistor Amplifier

A well-known property of common base transistor configuration is that its input impedance will exhibit an inductive component, as shown by Searle et al [15]. The hybrid-pi model is one of the various types of representations of the incremental behaviour of a transistor connected in the common base configuration shown in figure 2.1. The resistance r_e, usually referred to as the emitter resistance, describes the incremental relationship between the emitter base junction voltage and the emitter current. The base resistance r_x represents the effects of transverse voltage drops in the base region caused by the base current. The capacitance C_μ is the space charge capacitance of the reverse biased collector junction. α is an incremental common base short circuit current gain and is defined by

$$\alpha = \frac{\alpha_0}{1+j(\omega/\omega_\alpha)}$$

where the break frequency ω_α is :

$$\omega_\alpha = 1/(r_e C_\pi)$$

The coefficient α_o is usually called the low frequency common base short circuit current gain.

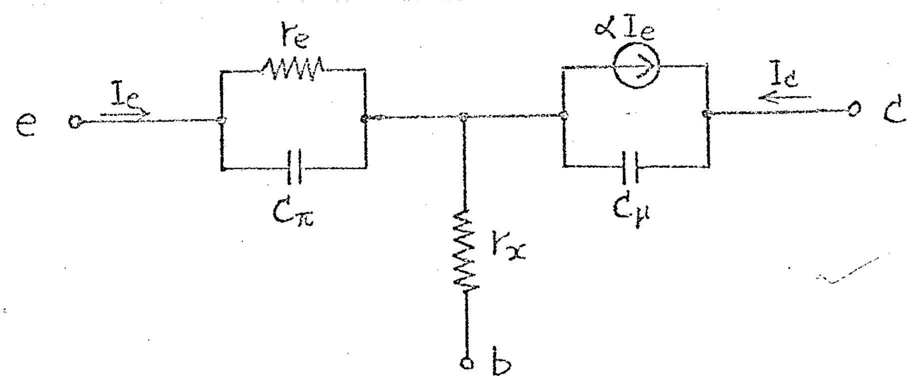

Figure 2.1 Common base T model equivalent circuit

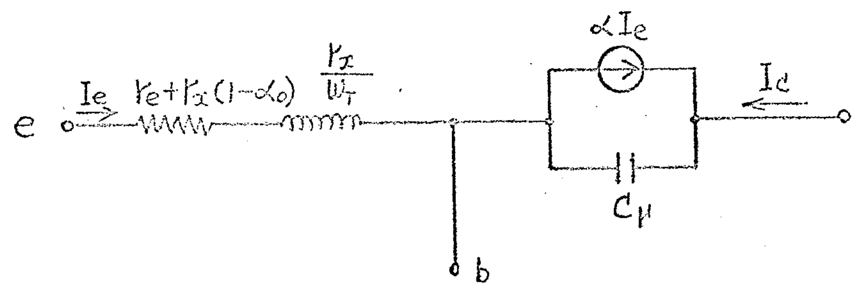

Firure 2.2 Approximate high frequency common base T model equivalent circuit

The modified common base T model is shown in figure 2.2, where $\omega_T = \frac{g_m}{C_\pi + C_\mu}$, and g_m is the incremental transconductance of a junction transistor. An external resistance R_b is shown in figure 2.3 connected to the base of the transistor and helps to increase the input inductance of the transistor circuit shown in figure 2.2.

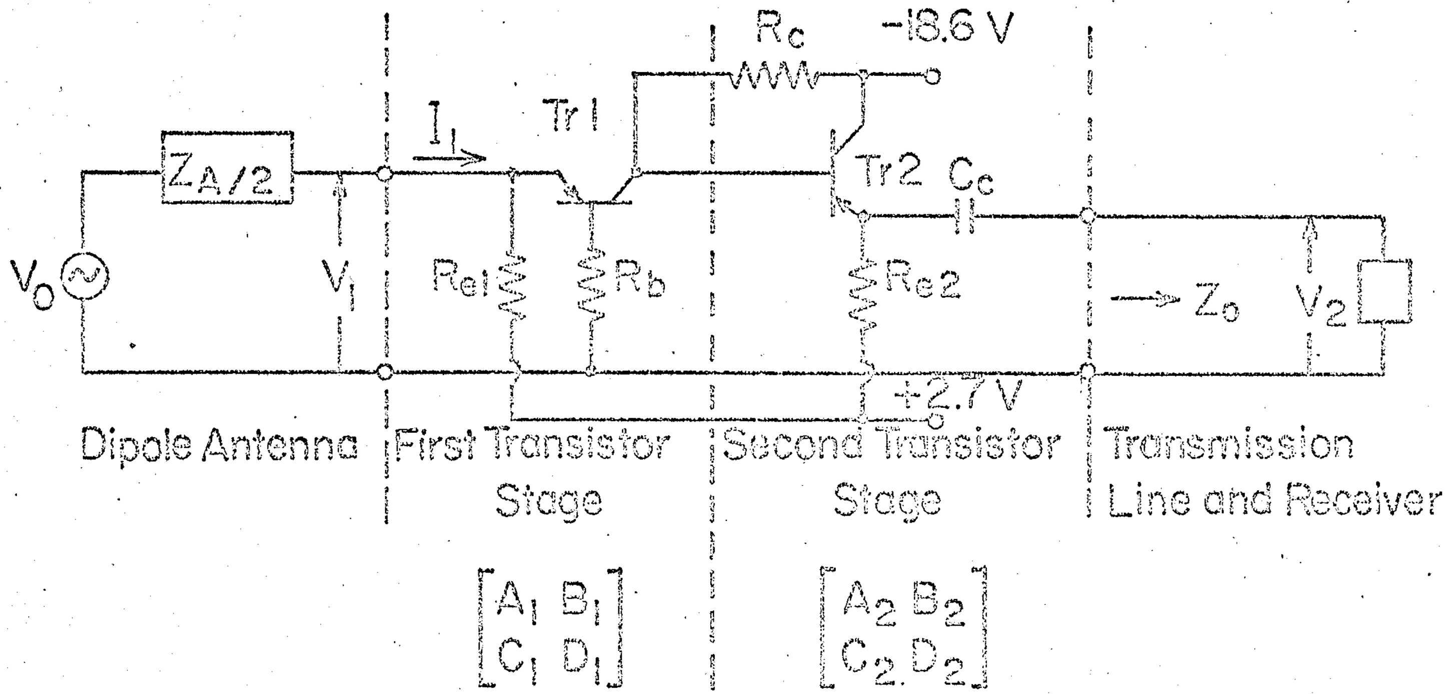

Figure 2.3. Equivalent circuit of active dipole antenna. $R_{e1} = 1K\Omega$, $R_{e2} = 5.6K\Omega$, $R_c = 4.7K\Omega$, $R_b = 150\Omega$, $C_c = 370pF$. T_{r1} and T_{r2} are Motorola 2N4959 transistors.

2.2 Equivalent Circuit of Transistor Amplifier

The transistor amplifier consists of two stages. The first stage, a common base configuration, is employed to investigate and exploit the inductive impedance property in order to improve the voltage gain and the bandwidth of the active dipole antenna. The first stage also serves to amplify the received voltage directly. The second transistor stage is a common collector circuit. It is employed as a current amplifier and is also used to provide an impedance match with the 50 ohm transmission line which is generally employed with high frequency receivers.

Conventional transistor circuit design can be facilitated through the use of two port network theory. The usefulness of this theory can be attributed to the fact that it is applicable to calculate the voltage gain, the input admittance and the output admittance of the transistor circuits employed in an active antenna. These calculations are made in terms of the short circuit Y admittance parameters, the open circuit Z impedance parameters, and the ABCD transmission parameters. The expressions required for relating these parameters may be found in Desoer and Kuh [16].

An equivalent transistor circuit is initially represented by the short circuit Y admittance parameters, since these may be easily measured or obtained from the manufacturer's data sheets. Nevertheless, it is conventional to convert the Y parameters into the Z parameters due to the presence of series elements such as R_b in the base of the first transistor stage shown in figure 2.3. The study of the conversion between the Z, Y and ABCD parameters is given in Appendices A and B.

For purposes of the analysis, the two-stage transistor amplifier may be considered as a cascaded network. The analysis is easily accomplished by using the ABCD parameters in the following calculations. The ABCD parameters are obtained from equations (B.1) to (B.4) given in Appendix B by using equations (A.1) to (A.3) given in Appendix A.

$$A_1 = \frac{Y_{22b} + R_b Y_b}{R_b Y_b - Y_{21b}} \qquad (2.1)$$

$$B_1 = \frac{A_1 (Y_{11b} + R_b Y_b)}{Y_b} - \frac{(R_b Y_b - Y_{12b})(R_b Y_b - Y_{21b})}{(R_b Y_b - Y_{21b}) Y_b} \qquad (2.2)$$

$$C_1 = \frac{A_1}{R_{e1}} + \frac{Y_b}{R_b Y_b - Y_{21b}} \qquad (2.3)$$

$$D_1 = \frac{B_1}{R_{e1}} + \frac{R_b Y_b + Y_{11b}}{R_b Y_b - Y_{21b}} \qquad (2.4)$$

where R_{e1} is the emitter resistor of the first stage shown in figure 2.3, and $Y_b = Y_{11b} Y_{22b} - Y_{12b} Y_{21b}$. The Y parameters refer to the short circuit admittance parameters of the common base or the common collector transistor when they are subscripted by b or c, respectively. The Y parameters and the subsequent ABCD parameters of the second stage transistor circuit, shown in figure 2.3, are derived in the same manner as those of the first stage, i.e.

$$A_2 = \frac{-1 - R_{e2}Y_{22c}}{R_{e2}Y_{21c}} \qquad (2.5)$$

$$B_2 = \frac{-1 - R_{e2}Y_{22c} - j\omega C_c R_{e2}}{j\omega C_c R_{e2} Y_{21c}} \qquad (2.6)$$

$$C_2 = \frac{-1 - Y_{22c}R_{e2} + R_c R_{e2} Y_c - Y_{11c}R_c}{R_c R_{e2} Y_{21c}} \qquad (2.7)$$

$$D_2 = \frac{-R_{e2}Y_{22c} + R_c R_{e2} Y_c - (1 + R_c Y_{11c})(1 + j\omega C_c R_{e2})}{j\omega C_c R_c R_{e2} Y_{21c}} \qquad (2.8)$$

where $Y_c = Y_{12c} Y_{21c} - Y_{11c} Y_{22c}$ while R_{e2}, C_c, and R_c are shown in figure 2.3.

From the property of the transmission parameters, the resulting transmission matrix of the two cascaded transistor stages is given by

$$\begin{bmatrix} A & B \\ C & D \end{bmatrix} = \begin{bmatrix} A_1 & B_1 \\ C_1 & D_1 \end{bmatrix} \begin{bmatrix} A_2 & B_2 \\ C_2 & D_2 \end{bmatrix} \qquad (2.9)$$

Using equation (2.9), the voltage gain and the input admittance of the transistor circuits are given by [17]

$$G_t = V_2 / V_1 = Z_0 / (AZ_0 + B) \qquad (2.10)$$

$$Y_t = I_1 / V_1 = (CZ_0 + D) / (AZ_0 + B) \qquad (2.11)$$

where $Z_0 = 50$ ohm while V_1, V_2, and I_1 are input voltage, output voltage, and input current of the transistor circuits, respectively, as shown in figure 2.3. The results of these computations are given in figures 3.7 and 3.8.

2.3 Equivalent Circuit of Passive Antenna

The Thevenin equivalent circuit of the passive monopole antenna is shown in figure 2.3 as a voltage source V_0 in series with an impedance $Z_A/2$ as given by Kraus [18]. The input impedance of a thin cylindrical monopole antenna is equal to one half of the impedance of a dipole antenna as shown by Jasik [19]. The input impedance $Z_A/2$ is calculated by applying the method of moments proposed by Harrington [20].

The calculated results of the input admittance are plotted as a function of frequency in figure 3.2.

2.4 Frequency Response of Active Antenna

The voltage gain of the active antenna is given by

$$G_a = V_2 / V_0 \qquad (2.12)$$

where V_0 is source voltage of the dipole antenna and V_2 is defined in section 2.2.

Since $V_1 = V_2$ in the absence of the transistor circuit shown in figure 2.3, the voltage gain of the passive antenna is given by

$$G_p = V_1 / V_0 = Z_0 / (Z_0 + Z_A/2) \qquad (2.13)$$

where Z_0 is the input impedance of the receiver, $Z_A/2$ is the input impedance of the passive antenna, and V_1 is defined in section 2.2. Figure 3.15 shows the relationship between G_a and G_p for the frequency range of 220 to 360 MHz.

The output admittance of the active antenna, as seen from the terminals of the transmission line, is denoted by Y_a and is computed from the expression

$$Y_a = (A + CZ_A/2) / (B + DZ_A/2) \qquad (2.14)$$

where A, B, C, and D are the elements of the active antenna given in equation (2.9) in matrix form.

2.5 Noise Temperature of Receiving System

The numerical examples given here are based on calculated and published values [12-14] with respect to the noise temperature of the receiving active and passive antenna systems. The noise behaviour of the passive antenna system T (in degrees Kelvin) may be expressed by [12]

$$T_p = T_E + T_R / G_L \qquad (2.15)$$

where T_E denotes atmospheric and man-made noise temperatures, T_R the noise temperature of the receiver, and G_L the available gain of the transmission line.

In the following numerical calculations, it is assumed that T_R=1400°K, G_L=0.5, and T_E=300°K as used by Meinke [12].

Substitution of these values in equation (2.15) leads to a plot of T_P versus frequency, as shown in figure 2.5.

The noise temperature of the receiving active antenna system T_a (in degrees Kelvin) is given by

$$T_a = T_E + T_T + T_R/(G_T G_L) \qquad (2.16)$$

where T_T and G_T are the noise temperature and the available gain of the transistor circuits, respectively.

Two port network theory is normally used to discuss the noise temperature of transistor circuits [21]. Figure 2.4 shows a noisy linear two port network. This network, with noise taken into account, can be represented by a noise free network with two noise generators added, i_{n1} and i_{n2}.

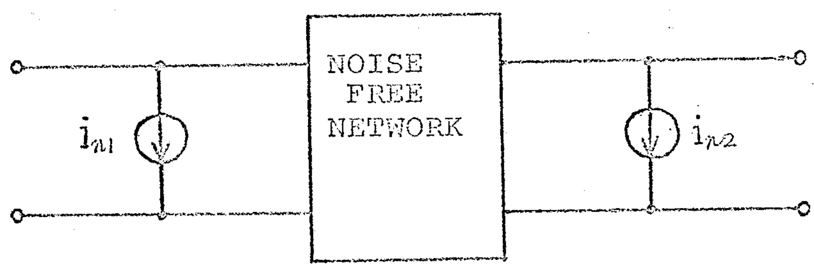

Figure 2.4 A noisy two port network using Y parameters

The input noise temperature of a two port network is defined by Sucher [22] as the temperature of the input termination which, when connected to a noise free equivalent network, would result in the same output noise power as that of the actual network connected to a noise free input termination. The input noise temperature T (in degrees Kelvin) is related to the noise factor F by

$$T=290(F-1) \qquad (2.17)$$

Using the Y parameters, the noise figure of a two port network is given by Vasseur [21] as

$$F=1+\frac{Re(Y_{11})}{Re(Y_g)}+\frac{Re(Y_{22})}{Re(Y_g)}\left|\frac{Y_{11}+Y_g}{Y_{21}}\right|^2-\frac{Re\left\{\frac{(Y_{11}+Y_g)(Y_{21}+Y_{12}^*)}{Y_{21}}\right\}}{Re(Y_g)} \qquad (2.18)$$

where Y_g is the source admittance. For the first stage, the Y parameters are defined by equations (2.1) to (2.4) and (A.4), and the source admittance Y_{g1} is given by

$$Y_{g1}=(R_{e1}+Z_A/2)/(R_{e1}Z_A/2) \qquad (2.19)$$

whereas for the second stage, the source admittance Y_{g2} is defined by

$$Y_{g2}=Y_{22b}-\frac{Y_{12b}Y_{21b}}{Y_{11b}+Y_{g1}}+\frac{1}{R_c} \qquad (2.20)$$

The overall noise figure of the active antenna is therefore

$$F=F_1+(F_2-1)/G_1 \qquad (2.21)$$

where F_1 and F_2, the noise figures of the first and the second transistor stages, are determined by substituting (2.19) and (2.20) into (2.18), respectively and G_1 is the available power gain of the first stage defined by

$$G_1=\frac{|Y_{21b}|^2 Re(Y_{g1})}{Re\{(Y_{11b}Y_{22b}-Y_{12b}Y_{21b}+Y_{22b}Y_{g1})(Y_{11b}^*+Y_{g1}^*)\}} \qquad (2.22)$$

The noise temperature of the receiving system of the active antenna is calculated from equations (2.15) to (2.22) and is shown in figure 2.5 as a function of frequency.

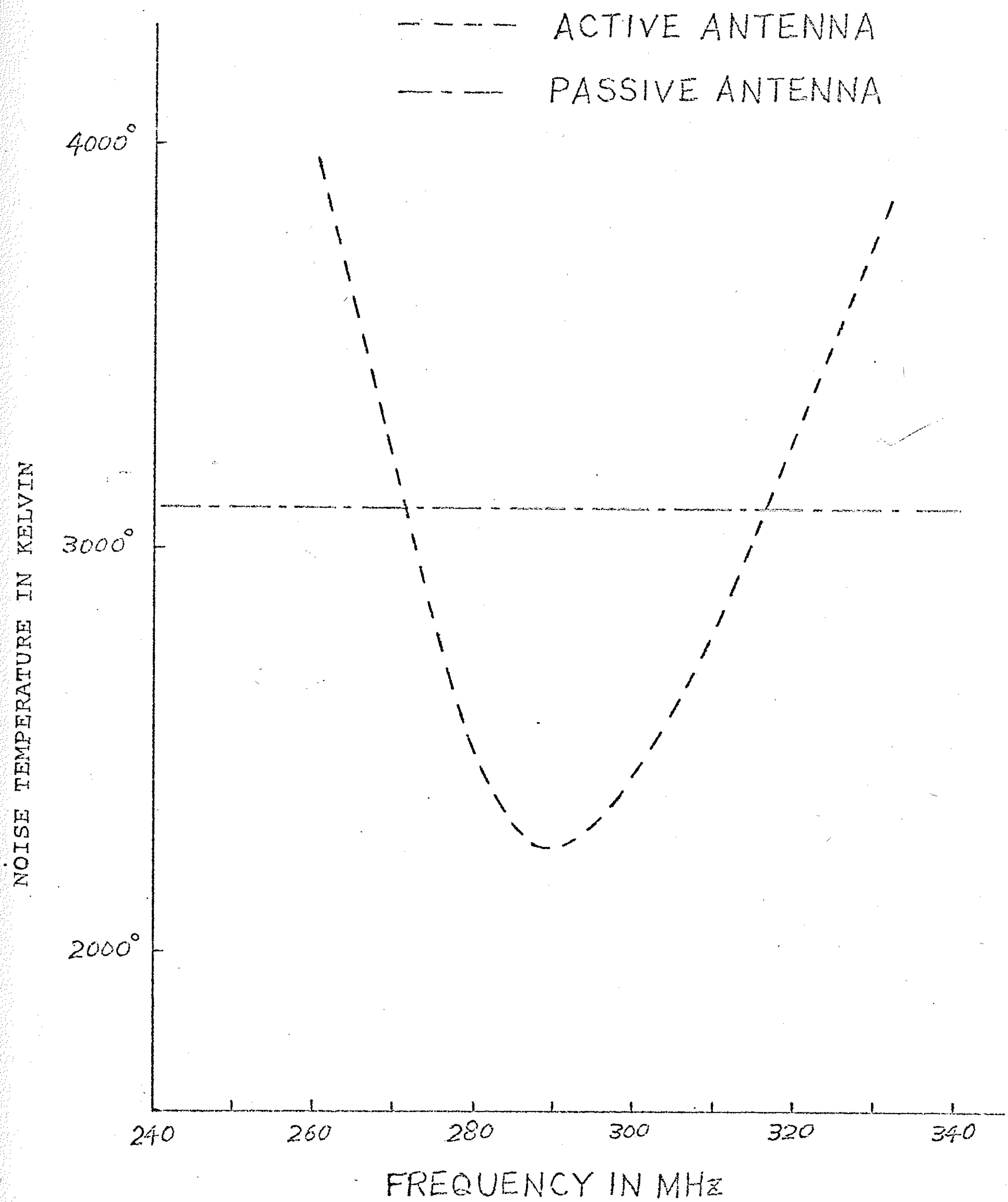

Figure 2.5. Noise temperature of the receiving system of the active and the passive antenna.

CHAPTER III

EXPERIMENTAL PROCEDURES AND RESULTS

In the previous chapter the circuit configurations of the active and the passive antennas were discussed. In this chapter the experimental measurements of the passive antenna input admittance, the transistor Y parameters, the input admittance of the transistor circuit, and the output admittance of the active antenna are presented. The gain of the active relative to the passive antenna is also discussed.

3.1 Input Admittance of Passive Antenna

The experiment was conducted in a large microwave anechoic chamber in the VHF and UHF ranges. The experimental setup for measuring the input admittance versus frequency is shown schematically in figure 3.1. The input admittance was conveniently measured by a General Radio Admittance Meter, Type 1602-B [23]. The apparatus consisted of a receiving monopole antenna over a ground plane, a signal generator, a local oscillator, a General Radio Admittance Meter, and a transmission line section of length D (distance between the terminal of the Admittance Meter and that of monopole antenna), as shown in figure 3.1.

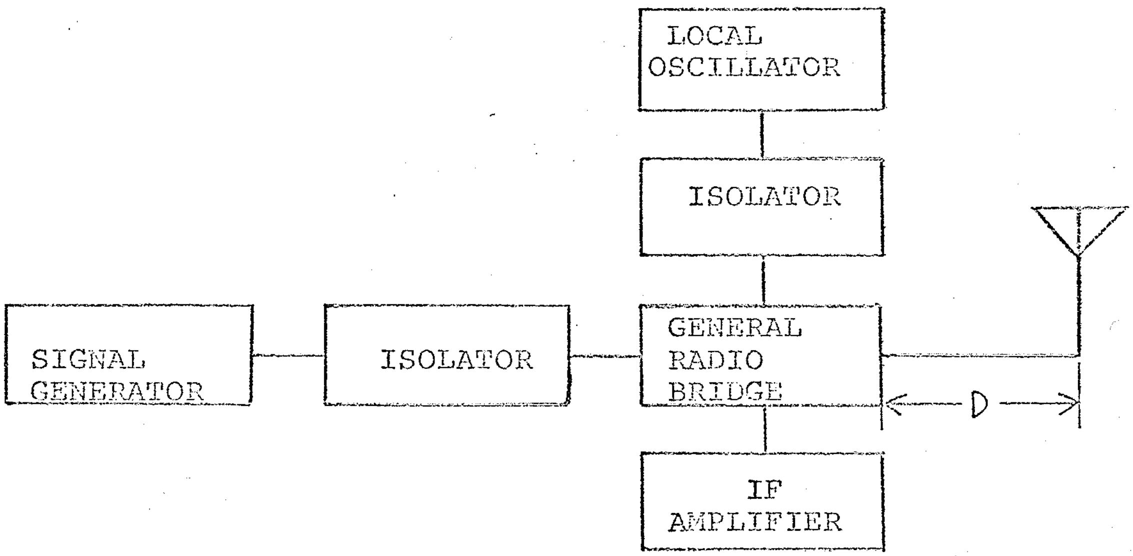

Figure 3.1 Circuit diagram for passive antenna input admittance measurements

If the transmission line is uniform, the over-all electrical length D is an integral multiple of a half wavelength, and the losses are negligible, then the unknown admittance is the same as the terminal admittance measured. The line length D was adjusted to the half wavelength value by means of a Type 874-LK20 Constant Impedance Adjustable Line and using various airlines inserted between the admittance meter and the antenna. For this adjustment, the line is short-circuited at the point at which the admittance is desired, the admittance meter set to balance at the admittance corresponding to a short circuit and the instrument balanced by adjusting the length of the line. It was found necessary to adjust the conductance arm on the instrument slightly in order to obtain a perfect null which would compensate for small losses and errors. The short circuit was then removed and the antenna, to be tested, was connected. The measured and computed data for a 23.3 cm long antenna are shown in figure 3.2.

The normalized admittance is given by

$$y=Y/20 \qquad (3.1)$$

where Y is the measured input admittance in millimhos for a 50 ohm line. The reflection coefficient Γ and VSWR are related to the normalized admittance y as follows

$$\Gamma=(1-y)/(1+y) \qquad (3.2)$$

$$VSWR=(1+|\Gamma|)/(1-|\Gamma|) \qquad (3.3)$$

The VSWR of the passive antenna is shown in figure 3.3.

3.2 Transistor Y Parameters

The Y parameters prove most useful for describing high frequency admittance devices and/or circuits. Knowing these parameters, all other electrical properties of the network can be derived.

The Y parameters of the Motorola 2N4959 transistors used were measured in the common base configuration using a General Radio Transfer Function and Immittance Bridge, Type 1607-A [24]. The experimental setup is shown in figure 3.4.

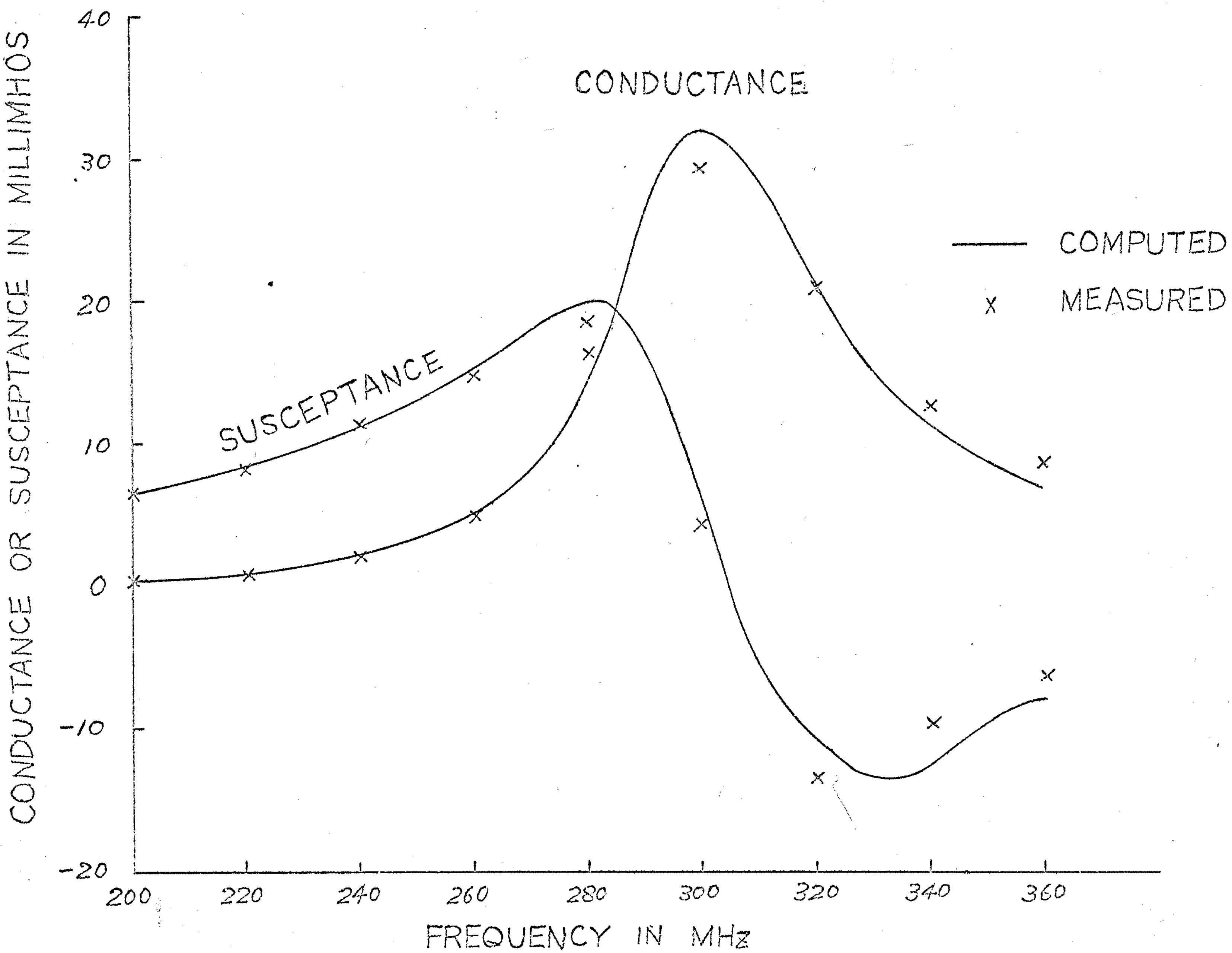

Figure 3.2. Input admittance of passive antenna.

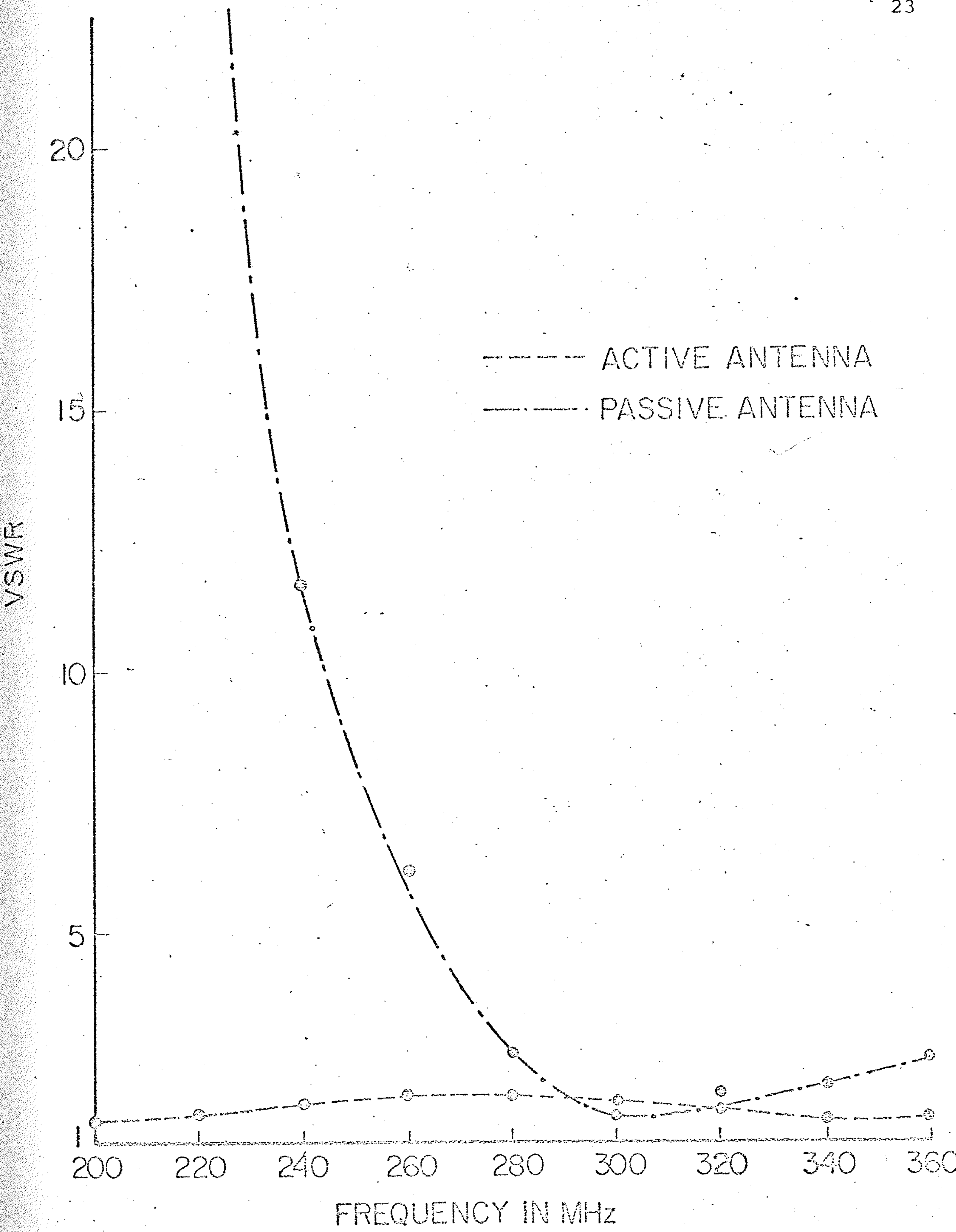

Figure 3.3. VSWR vs. frequency.

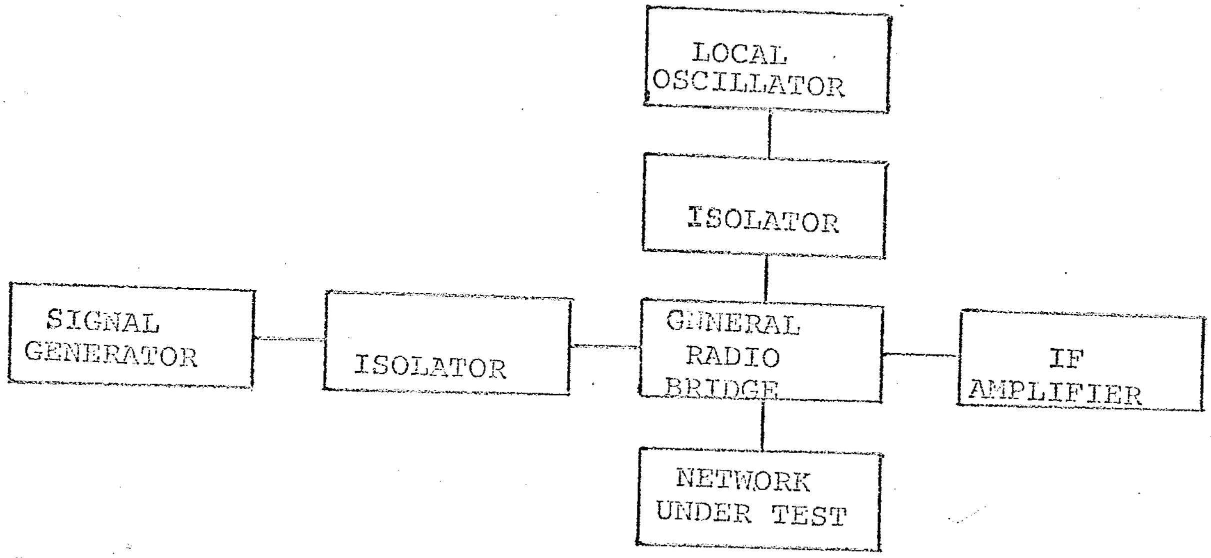

Figure 3.4 Circuit diagram for measurement of Y parameters

The input admittance Y_{11b} and the output admittance Y_{22b} are measured for a bias of 2mA emitter current and 10 V_{CE} in the frequency range between 200-360 MHz by steps of 20 MHz. Y_{12b} is obtained from Motorola data sheets since it is very hard to measure accurately. The magnitude of Y_{12b} is generally very small compared to the other parameters.

Transadmittance parameters Y_{12b} are measured using the Transfer Function Indicator of the Bridge in the same bias condition as Y_{11b} and Y_{22b}. The polynomial equations of the measured Y parameters (in millimhos) in the common base configuration are obtained by a computer curve fitting program. The resulting equations are:

$Y_{11b} = 76.4 - 0.1353f + 1.335f^2 10^{-4} + j(-10.022$

$$-4.182f10^{-2}+1.734f^{2}10^{-5}) \quad (3.4)$$

$$Y_{12b}=j(-0.03271-9.67f10^{-4}-1.974f^{2}10^{-7}) \quad (3.5)$$

$$Y_{21b}=-73.61+0.1418f-1.1f^{2}10^{-4}+j(16.65$$

$$+0.03378f+1.025f^{2}10^{-5}) \quad (3.6)$$

$$Y_{22b}=0.8962-4.151f10^{-3}-6.855f^{2}10^{-6}+3.308f^{3}10^{-8}$$

$$+1.188f^{4}10^{-11}+3.295f^{5}10^{-13}-9.463f^{6}10^{-16}$$

$$+j(3.738-2.075f10^{-2}+5.108f^{2}10^{-5}) \quad (3.7)$$

where f is the operating frequency varying from 200 to 360 MHz.

The common collector Y parameters (in millimhos) are calculated from the common base Y parameters using equations (c.1) to (c.4) given in Appendix C. The resulting polynomial equations are given by

$$Y_{11c}=3.328+2.67f10^{-3}+3.129f^{2}10^{-5}+j(10.11$$

$$-0.02951f+7.82f^{2}10^{-5}) \quad (3.8)$$

$$Y_{12c}=-2.82-6.058f10^{-3}-2.42f^{2}10^{-5}+j(-6.402$$

$$+7.751f10^{-3}-2.73f^{2}10^{-5}) \quad (3.9)$$

$$Y_{21c}=-76.4+0.1353f-1.335f^{2}10^{-4}+j(10.26$$

$$+0.0426f-1.705f^{2}10^{-5}) \quad (3.10)$$

$$Y_{22c}=76.4-0.1353f+1.335f^{2}10^{-4}+j(-10.22$$

$$-0.04182f+1.734f^{2}10^{-5}) \quad (3.11)$$

3.3 Input Admittance and Gain of the Transistor Circuit

The two-stage transistor circuit for the active antenna

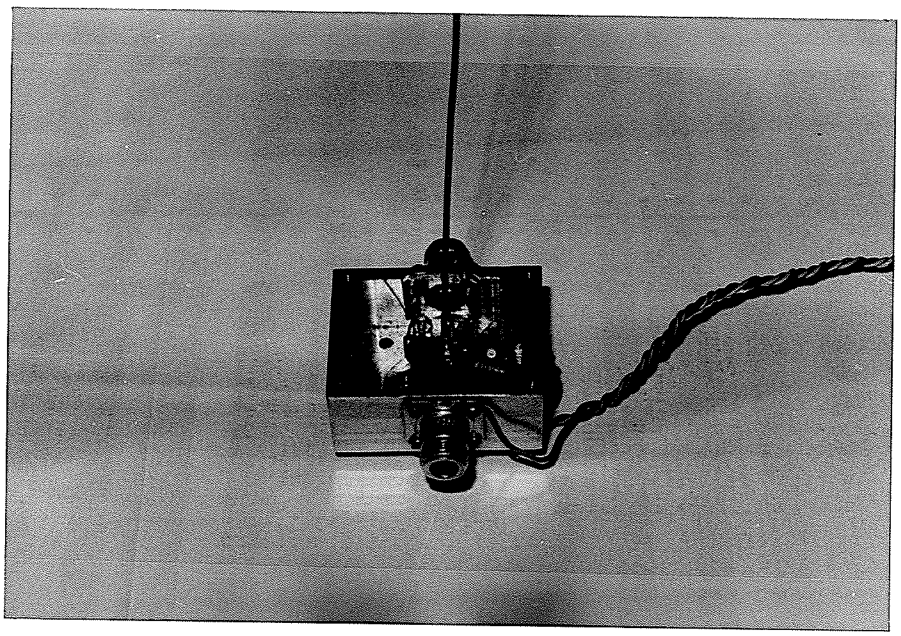

Figure 3.5. Photograph of active dipole antenna.

is shown in figure 2.3. The circuit was carefully wired to minimize the length of all leads in order to obtain good high frequency performance. Figure 3.5 shows the actual prototype of the active antenna.

The input admittance of the transistor circuit was measured by a General Radio Transfer Function and Immittance Bridge, Type 1607-A [24]. The circuit diagram and measured data are shown in figures 3.6 and 3.7, respectively.

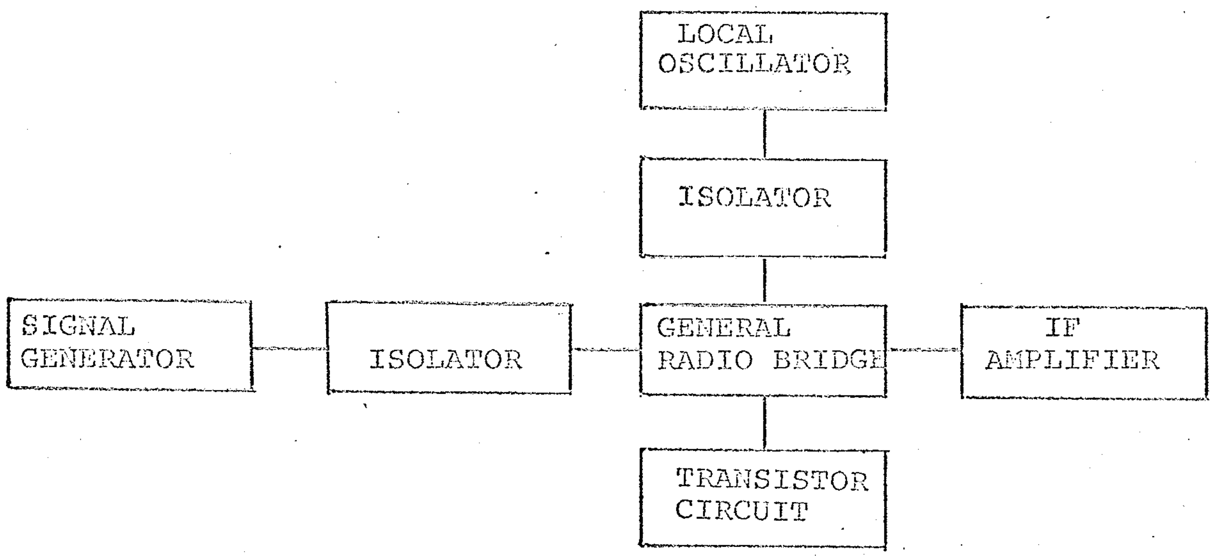

Figure 3.6 Circuit diagram for measurement of input admittance

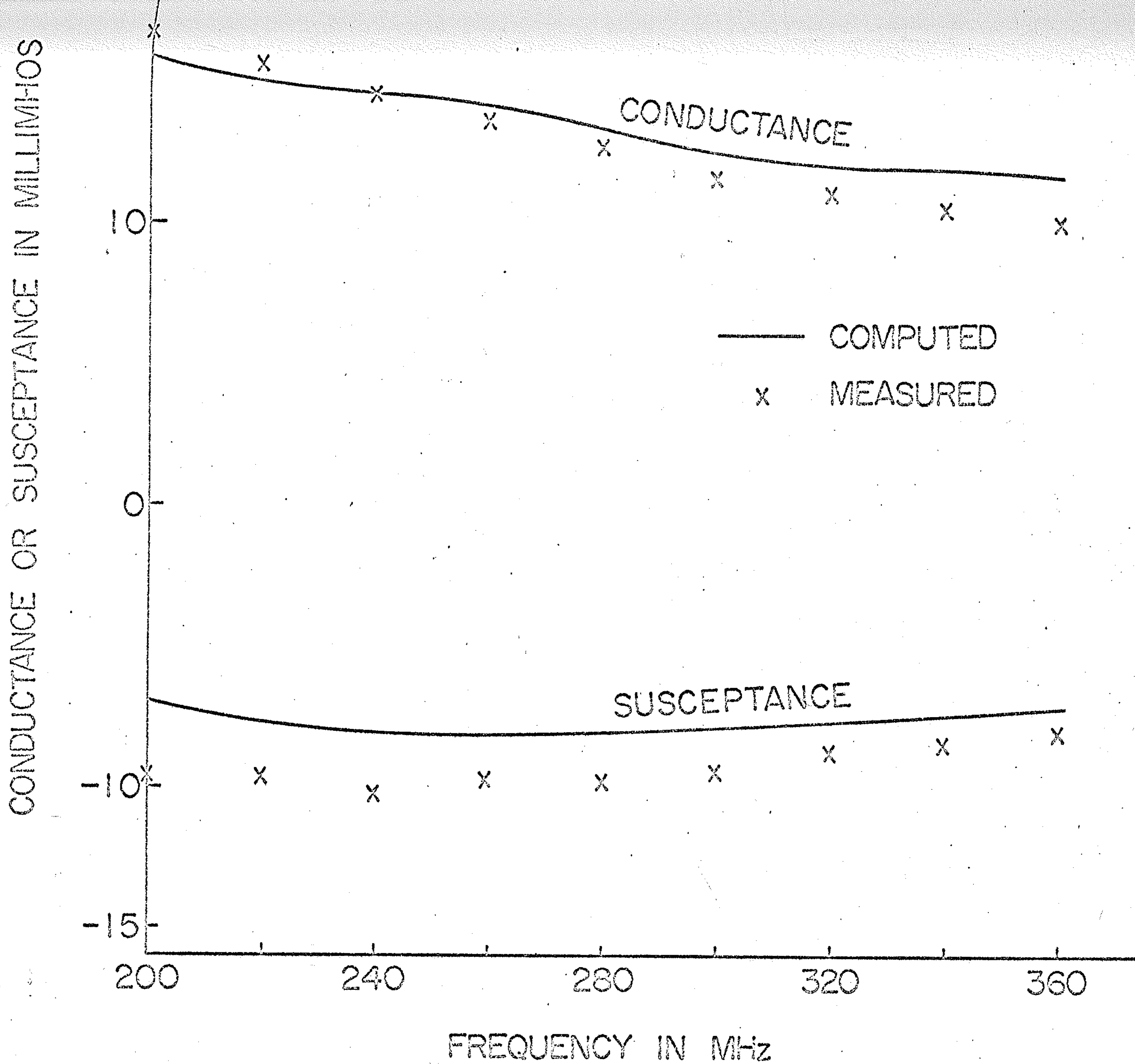

Figure 3.7. Input admittance of transistor circuit vs. frequency.

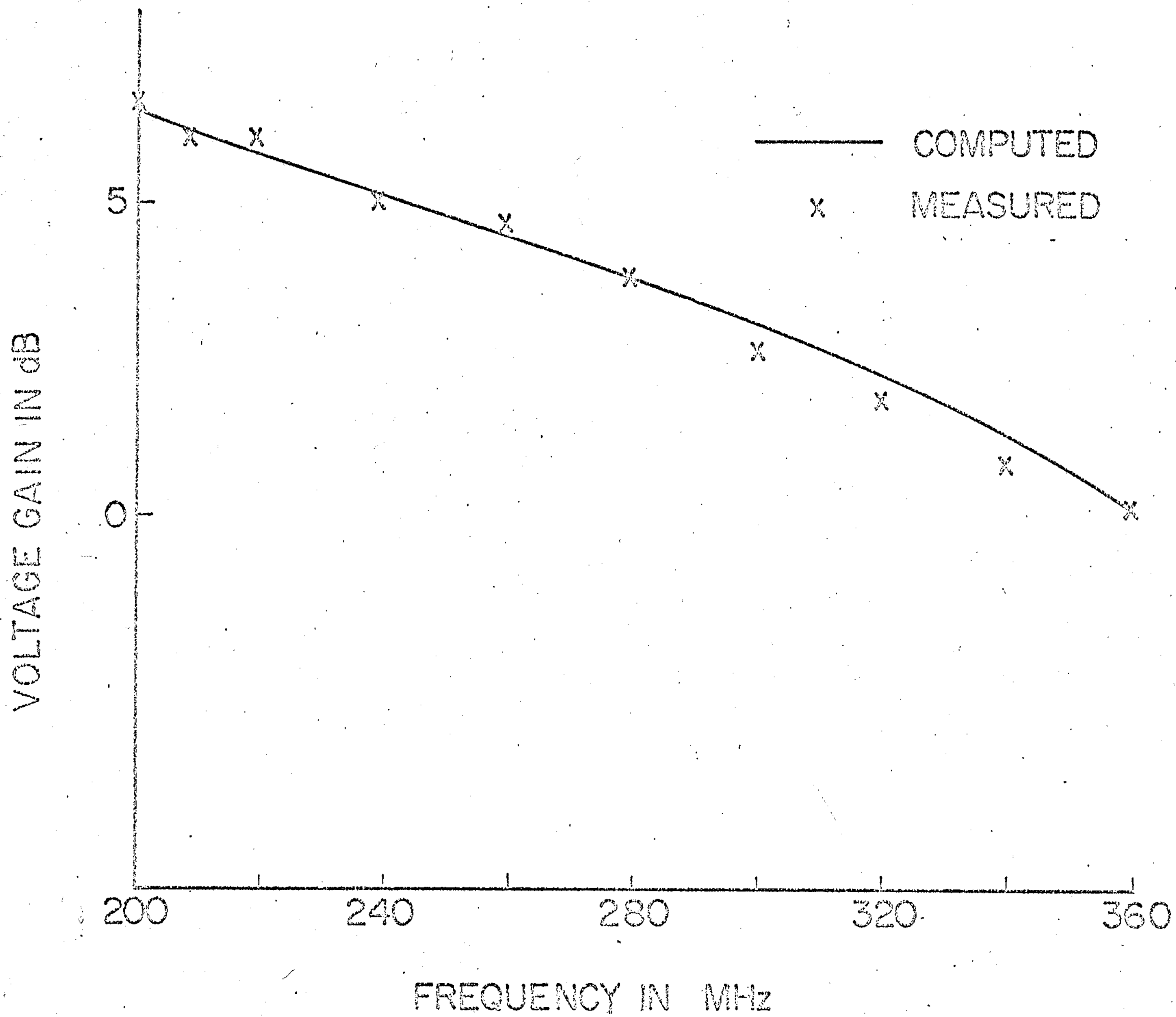

Figure 3.8. Transistor amplifier gain vs. frequency.

The voltage gain of a transistor circuit is denoted by V_2/V_1 and is shown in figure 3.8. The voltage gain was measured using a Hewlett Packard Vector Voltmeter, model 8405A, while the calculated gain was based on the Y parameters specified by the manufacturer of the Motorola 2N4959 transistors.

3.4 Output Admittance of Active Antenna

The experiment was conducted in a large microwave anechoic chamber. The experimental setup for measuring the output admittance versus frequency is shown schematically in figure 3.9. Figure 3.11 and 3.10 show the photographs of the transmitting antenna and apparatus, respectively.

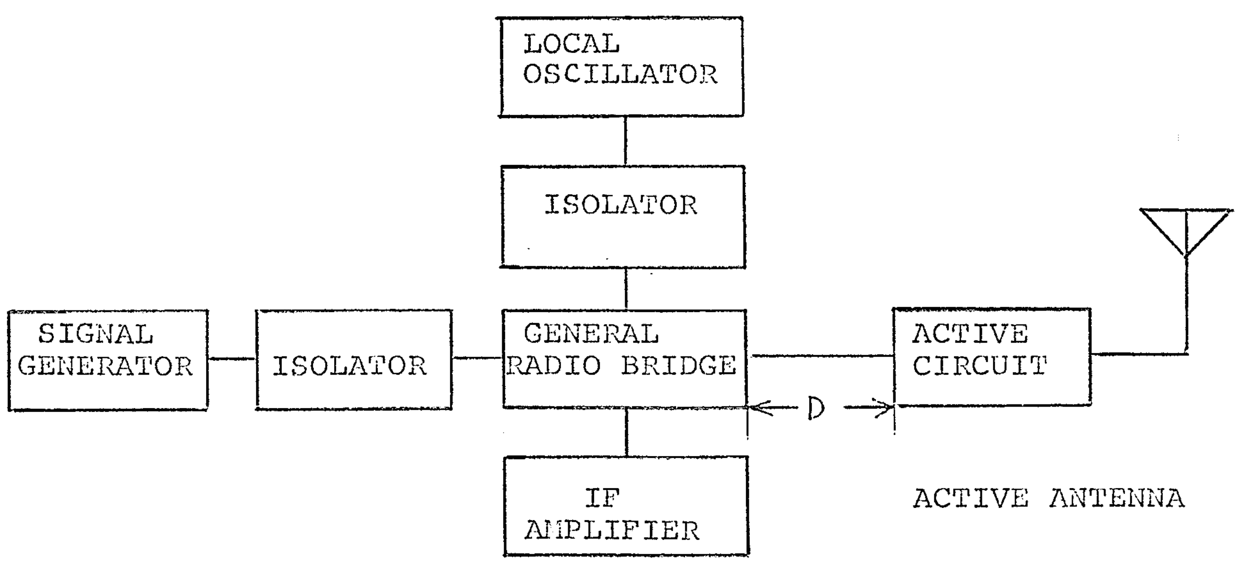

Figure 3.9 Circuit diagram for measuring the output admittance of the active antenna

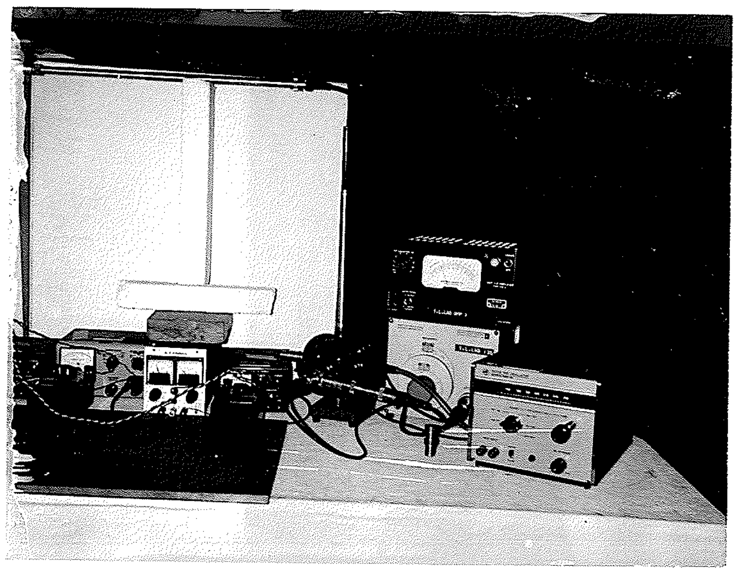

Figure 3.10. Setup for measuring the output admittance of the active antenna.

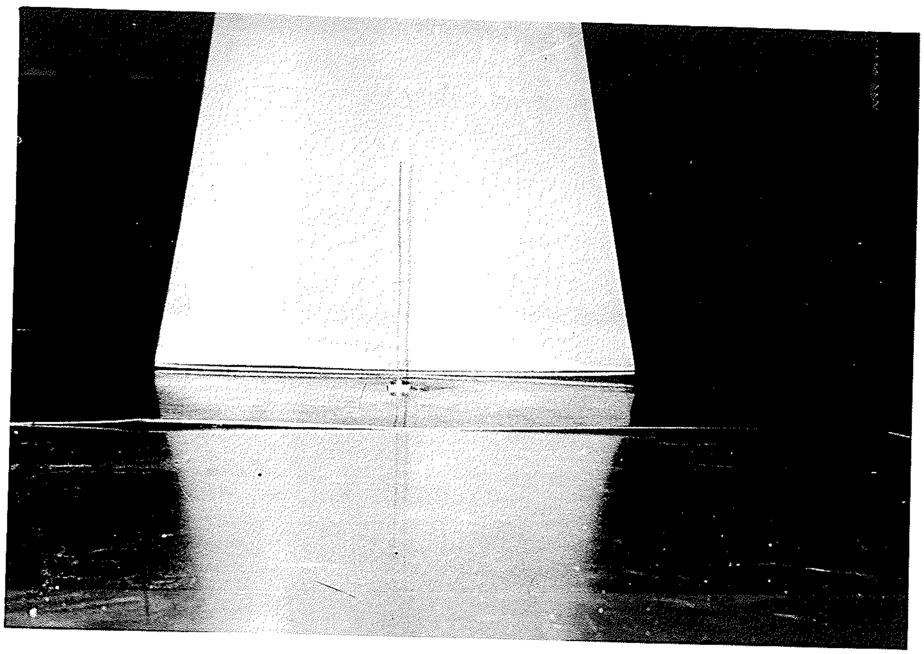

Figure 3.11. Photograph of transmitting antenna.

The measuring technique is the same as that described in section 3.1 for input admittance of the passive antenna. The VSWR of the active antenna is calculated from measurements of the output admittance using equations (3-1) to (3-3), and it is shown in figure 3.3.

3.5 Relative Gain

The apparatus for determining the relative gain consists of transmitting and receiving monopoles over a ground plane as shown in figure 3.11. The heights of transmitting and receiving monopoles are 32.0 and 22.4 cm, respectively, while the radius of these is 1.8 mm. Photographs of trasmitting antenna and apparatus are shown in figures 3.12 and 3.13.

The equipment assembly was situated in a large microwave anechoic chamber which is adequate above 200 MHz. The generator frequency was varied from 220 to 360 MHz in steps of 20 MHz. The experimental setup for relative receiving gain measurements is shown in figure 3.14. The incident voltage V as shown in figure 3.14, was maintained at a constant level throughout the test while the reflected voltage V as shown in figure 3.14, was minimized by tuning the adjustable stubs at each frequency. The voltages V and V given in figure 3.14, received at the terminals of the passive and active dipoles were measured at each frequency using a Hewlett Packard Vector Voltmeter, model 8405A, as

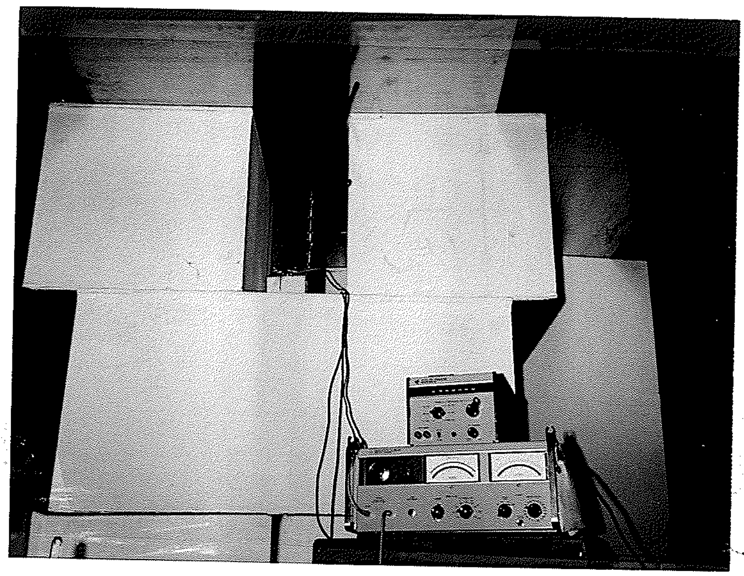

Figure 3.12. Photograph of some equipment associated with the transmitting antenna. (Signal Generator, Double Stub Tuner and Vector Voltmeter.)

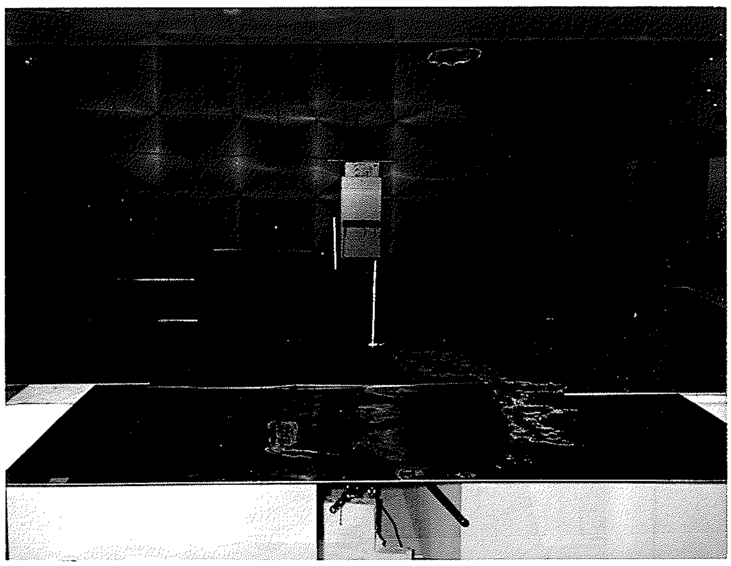

Figure 3.13. Photograph of experimental setup for transmitting and receiving antennas.

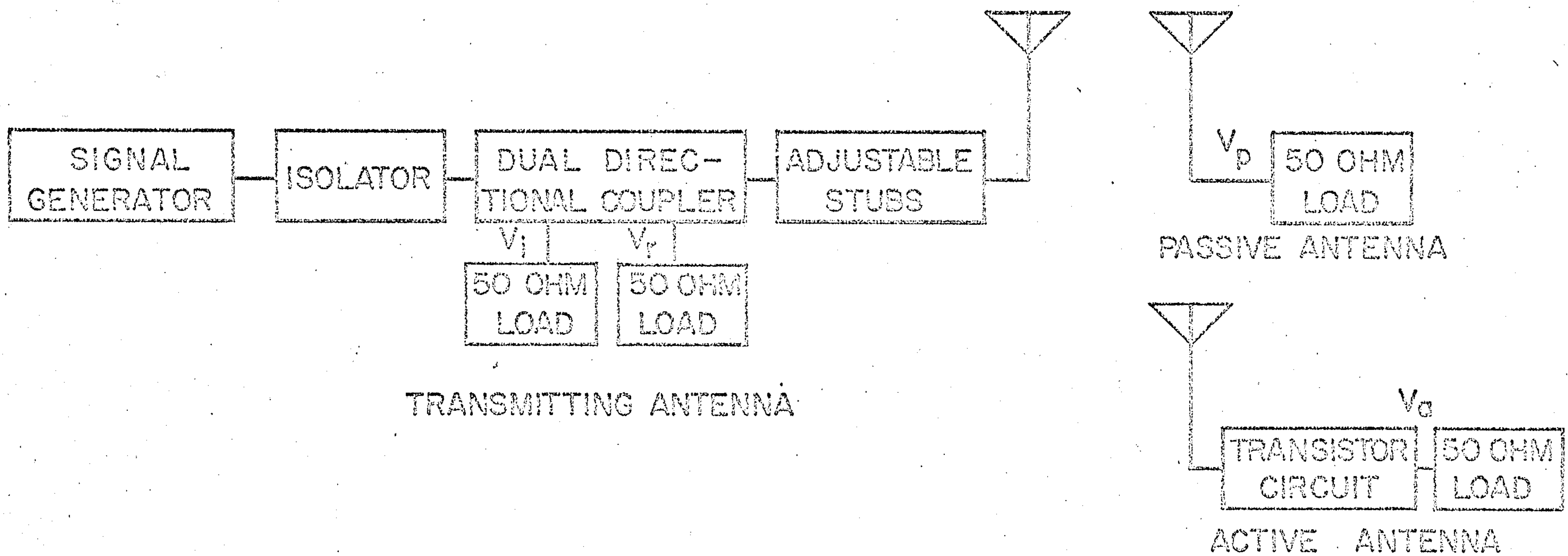

Figure 3.14. Experimental setup for relative receiving gain measurement.

shown in figure 3.12. The difference in the gain of the receiving passive and active dipoles as a function of frequency is shown in figure 3.15.

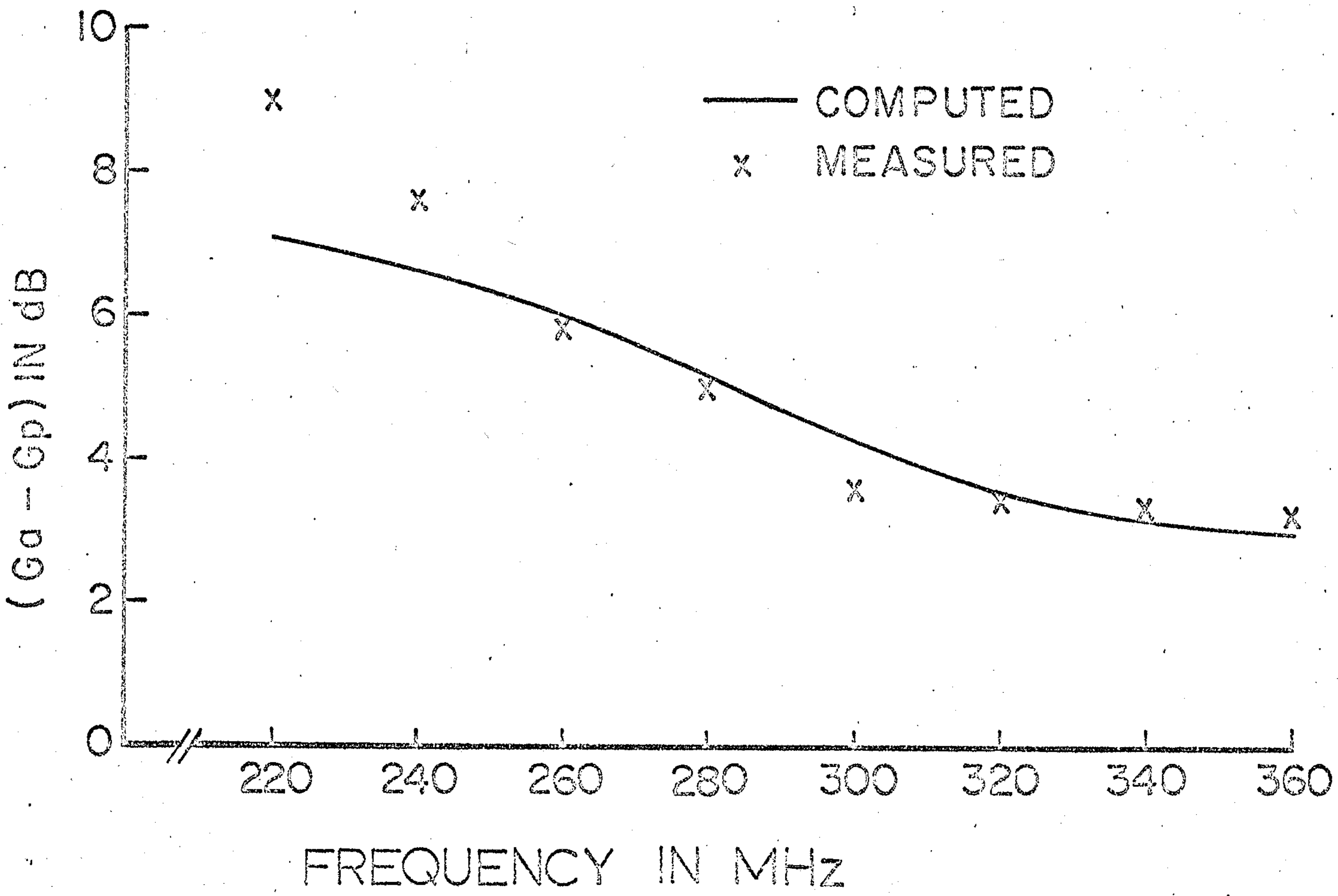

Figure 3.15. $G_a - G_p$ vs. frequency.

CHAPTER IV

DISCUSSION AND CONCLUSIONS

4.1 Discussion of the Results

Examination between the theory and the experiment for input admittance and voltage gain of the transistor circuit as a function of frequency indicates good agreement shown in Figure 3.7 and 3.8. These results confirm the basic idea of using a transistor amplifier with inductive input impedance for conjugate matching of the dipole antenna over an appreciable frequency range.

Figure 2.4 shows that the noise temperature of the receiving active antenna system is lower than that of the passive antenna system over the 273-313 MHz range by a maximum of 835 K at 290 MHz. Figure 3.3 shows that the VSWR as a function of frequency of the active antenna is 1.4 to 1.9 and considerably lower than that of the passive antenna, particularly for lower frequencies. Figure 3.15 shows that the improvement in the gain of the active antenna over the passive one in the 220-360 MHz range lies between 3 and 9 dB approximately, where the larger improvements correspond to lower frequencies.

The above improvements compare favourably with previous results reported by Landstorfer [14] who found that the noise temperature of the receiving active antenna system was

1470 K at 475 MHz. The VSWR of the active antenna tested by Meinke [12] is less than 2.5 in the frequency range of 2.5 to 25 MHz, indicating a similar VSWR result.

The bandwidth of the active dipole antenna is larger than that of the passive one by approximately 10 % for a value R equal to 150 ohms used in the experiment, as shown in figure 4.1. The calculated curves given in this figure indicate the significance of R for controlling the bandwidth and the gain as well as for lowering the center frequency of the active antenna.

The theoretical results in all cases agree favourably with experimental data except for a few points in the gain-frequency curve as shown in figure 3.15. This discrepancy may be attributed to circuit wiring as well as approximations in computing the antenna input admittance and in taking the measurements described in chapter III.

4.2 Conclusions

In this thesis a technique for improving the bandwidth and the receiving gain of a passive dipole antenna of the same length has been presented, by introducing a specially designed transistor circuit which presents an inductive reactance to the antenna and amplifies the received voltage. The active antenna has been shown to have a higher gain and

Curve	Dipole Type	R_b(OHMS)	Q	Dipole Gain(dB)	Centre Frequency(MHz)
I.	Passive	—	2.34	−4.16	288
II.	Active	150	1.99	1.10	266
III	Active	300	1.25	−1.68	250
IV	Active	450	1.01	−3.36	240

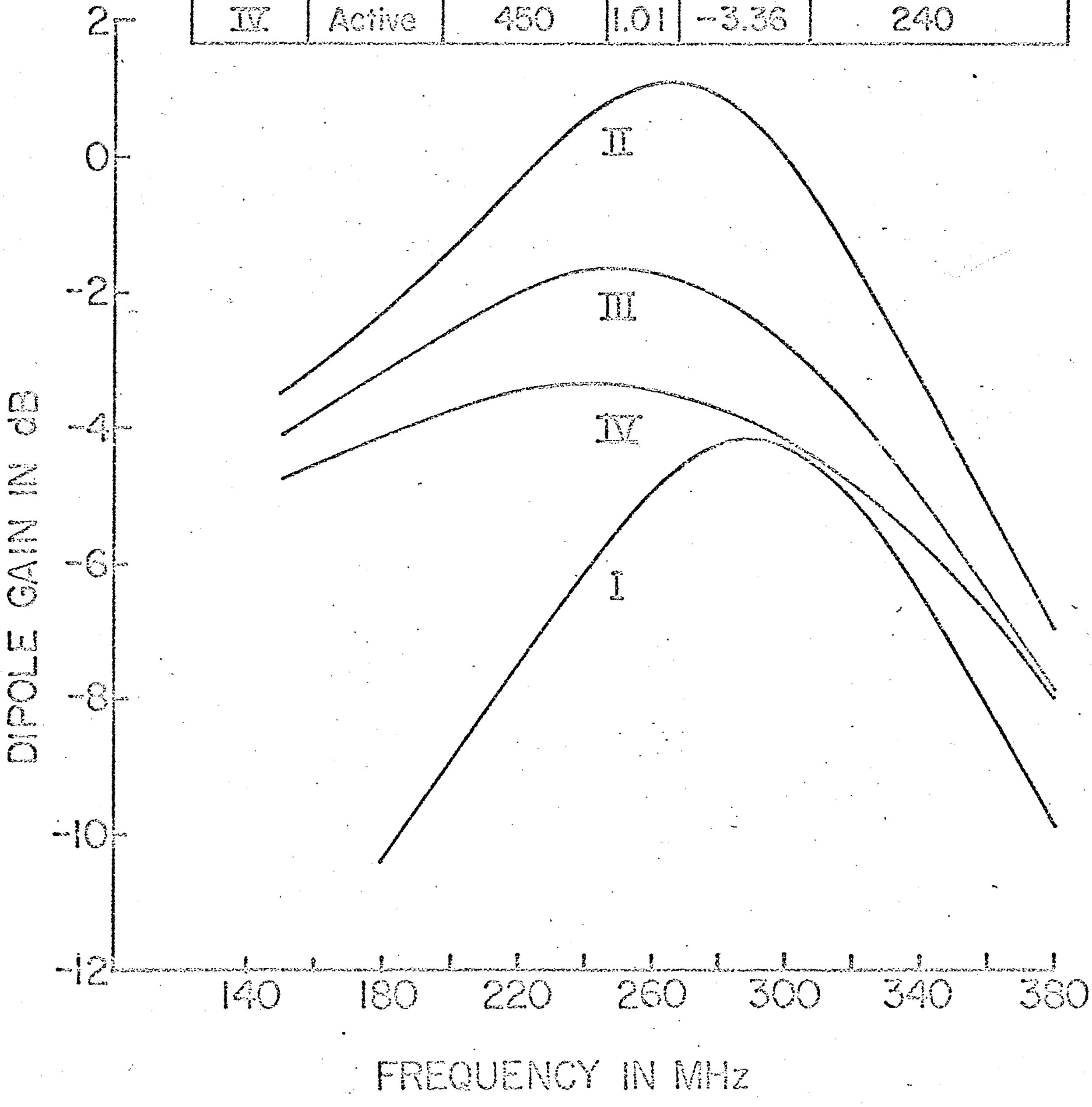

Figure 4.1. Dipole gain vs. frequency. All curves correspond to receiving dipoles of 1.8 mm radius and 44.8 cm tip to tip.

a larger bandwidth than the passive antenna while the noise temperature of the receiving active antenna system is lower than that of the passive antenna system over a limited frequency range. Since for a given frequency, the value of the noise temperature of the active antenna receiving system is dependent on the noise of the transistor used, a further improvement of the active antenna noise is possible with low noise transistors. The center frequency of the active antenna is, however, lower than that of the passive antenna. This fact can be effectively used to reduce the physical or electrical length of a passive antenna without sacrificing its electrical performance. The frequency response of an active antenna, the center frequency and the maximum gain decrease, while the bandwidth increases, with increasing values of the base registor R

The advantages of integrated circuits for antennas are greater simplicity, increased reliability, smaller size and weight and improved electrical performance. These features are of considerable importance in broadcasting as well as in satellite and space vechile applications.

4.3 Suggestions for Future Research

In this thesis an active antenna system was employed as a single unit; however, it is possible to utilize multiple units to construct active antenna arrays with elements whose gain can be controlled independently as a function of center frequency. In such arrays also the bandwidth can be controlled electronically by varying the base registor R

As a results of its inherent properties, the active antenna can be utilized for control of gain and half power beamwidth as well as for low power transmission [25].

There are many types of matching networks for active antennas. These networks comprise not only common base transistor circuits, but also negative impedance converters [26-29] and inverted common collector circuits [30-31]. Active antennas using negative impedance converters and inverted common collector circuits may possibly achieve larger gain, larger bandwidth, and lower center frequency than these of common base circuits employed in this thesis.

BIBLIOGRAPHY

1. Fujimoto, K., "Active Antenna," Television in Japan, Vol. 22, No. 2, pp94-99, February, 1968.

2. Hansen, R.C., "Special Issue on Active and Adaptive Antenna," Proc. IEEE., AP-12, No. 2, pp140-141, March, 1964.

3. Frost, A.D., "Parametric Amplifier Antenna," Proc. IRE., Vol. 48, pp1163-1164, June, 1960.

4. Frost, A.D., "Parametric Amplifier Antenna," IEEE Trans., Vol. AP-12, No. 2, pp234-236, March, 1964.

5. Fujimoto, K., "Tunnel-Diode-Loaded-Dipole Antenna," IEEE trans., Vol. AS-2, pp297-307, April, 1964.

6. Fujimoto, K., "Active Antennas : Tunnel-Diode-Loaded Dipoles," Proc. IEEE, Vol. 53, No. 2, pp174, February, 1965.

7. Fujimoto, K., "Active Dipole Antennas with Esaki Diodes," Electronics & Communications Engineers in Japan, Vol. 48, No. 4, pp255-265, April, 1965.

8. Meinke, H.H., "Tunnel Diodes Integrated with Microwave Antenna Systems," The Radio and Electronics Engineer, Vol. 31, No. 2, pp76-80, February, 1966.

9. Copeland, J.R. and Robertson, W.J., "Design of Antennaverters and Antennafiers," Electronics, Vol. 34, pp68-71, October, 1961.

10. Copeland, J.R., Robertson, W.J. and Verstraete, R.G., "Antennafier Arrays," IEEE trans., Vol. AP-12, No. 2, pp227-233, March, 1964.

11. Furukawa, I., Hamid, M.A.K. and Yunik, M., "Frequency Response of Active Dipole Antennas," to be published International Journal of Elecronics.

12. Meinke, H.H., "Transistorized Receiving Antennas," Progress Report No. 6 to Air Force Avionics Laboratory, U.S. Air Force, Contract No. AF 61(052)-950.

13. Meinke, H.H., and Landstorfer, F.M., "Noise and Bandwidth Limitations with Transistorized Antennas," 1968 G-AP International Symposium, Boston, Mass., pp245-246, 1968.

14. Landstorfer, F.M., "Applications and Limitations of Active Aerials at Microwave Frequencies," European Microwave Conferece, IEE London, pp141-144, September, 1969.

15. Searle, C.L., et al, "Elementary Circuit Properties of Transistors," SEEC Vol. 3, John Wiley & Sons, pp216, 1964.

16. Desoer, C.A. and Kuh, E.S., "Basic Circuit Theory," McGraw-Hill, pp747, 1969.

17. Ghausi, M.S., "Principles and Design of Linear Active Circuits," McGraw-Hill, pp52, 1965.

18. Kraus, J.D., "Antenna," McGraw-Hill, pp42, 1950.

19. Jasik, H., "Antenna Engineering Handbook," McGraw-Hill, chap. 3, 1961.

20. Harrington, R.F., "Field Computation by Moment Methods," Macmillan Co., pp62-72, 1968.

21. Vasseur, J.P., "Properties and Applications of Transistors," Macmillan Co., pp377-392, 1964.

22. Sucher, M. and Fox. J., "Handbook of Microwave Measurements," Polytechnic Press of the Polytechnic Institute of Brooklyn, chap. 17, 1963.

23. Operating Instructions, Type 1602-B Admittance Meter, Form 741-F, General Radio Co., 1958.

24. Operating Instructions, Type 1607-A Transfer-Function and Immitance Bridge, Form 1607-0100-F, General Radio Co., 1964.

25. Copeland, J.R., and Robertson, W.J., "Antennas have Built-in Circuit," Electronic Engineer, pp115-120, May, 1963.

26. Linvill, J.G., "Transistor Negative-Impedance Converters," Proc. IRE, Vol. 47, No. 6, pp725-729, June, 1959.

27. Merrill, J.L.Jr., "Theory of the Negative Impedance Converter," Bell Sys. Tech. Jour., Vol. 30, pp88-109, January, 1951.

28. Ruston, H. and Bordogna, J., "Electric Networks : Functions, Filters, Analysis," McGraw-Hill, pp239-244,

1966.

29. Ghausi, M.S., "Principles and Design of Linear Active Circuits," McGraw-Hill, pp526-529, 1965.

30. Archer, J.A., Gibbons, J.F., and Purnaiya, G.M., "Using of Transistor-Simulated Inductance as an Interstage Element in Broadband Amplifiers," IEEE Journal of Solid-State Circuits, Vol. SC-3, No. 1, pp12-21, March, 1968.

31. Dill, H.G., "Inductance Semiconductor Elements and Their Application in Bandpass Amplifiers," IRE Trans. on Military Electronics, Vol. MIL-5, pp239-250, July, 1961.

APPENDIX A

CONVERSION BETWEEN Z, Y, AND ABCD PARAMETERS

The conversion from Z to Y parameters is given by

$$Y_{11}=Z_{22}/\Delta z,\quad Y_{12}=-Z_{12}/\Delta z,\quad Y_{21}=-Z_{21}/\Delta z$$

$$Y_{22}=Z_{11}/\Delta z \qquad (A.1)$$

where $\Delta z=Z_{11}Z_{22}-Z_{12}Z_{21}$.

The conversion from Y to Z parameters is given by

$$Z_{11}=Y_{22}/\Delta y,\quad Z_{12}=-Y_{12}/\Delta y,\quad Z_{21}=-Y_{21}/\Delta y$$

$$Z_{22}=Y_{11}/\Delta y \qquad (A.2)$$

where $\Delta y=Y_{11}Y_{22}-Y_{12}Y_{21}$.

The conversion from Y to ABCD parameters is given by

$$A=-Y_{22}/Y_{21},\quad B=-1/Y_{21},\quad C=-\Delta y/Y_{21}$$

$$D=-Y_{11}/Y_{21} \qquad (A.3)$$

The conversion from ABCD to Y parameters is given by

$$Y_{11}=D/B,\quad Y_{12}=-\Delta abcd/B,\quad Y_{21}=-1/B,\quad Y_{22}=A/B \qquad (A.4)$$

where $\Delta abcd=AD-BC$.

APPENDIX B

CONVERSION FROM Z TO ABCD PARAMETERS FOR THE FIRST TRANSISTOR CIRCUIT

The representation of the first transistor stage in terms of Z parameters is shown in figure B.1.

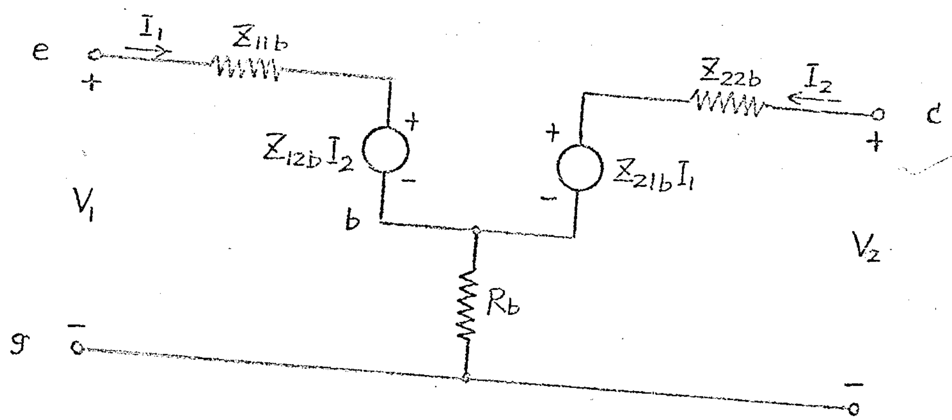

Figure B.1 First stage equivalent transistor circuit using Z parameters

The resulting equivalent circuit can be further modified as shown in figure B.2, using the relationships shown below.

$$Z'_{11b} = \frac{V_1}{I_1}\bigg|_{I_2=0} = \frac{I_1 Z_{11b} + I_2 Z_{12b} + R_b(I_1+I_2)}{I_1}\bigg|_{I_2=0} = Z_{11b} + R_b \qquad (B.1)$$

$$Z'_{12b} = \frac{V_1}{I_2}\bigg|_{I_1=0} = \frac{I_1 Z_{11b} + I_2 Z_{12b} + R_b(I_1+I_2)}{I_2}\bigg|_{I_1=0} = Z_{12b} + R_b \qquad (B.2)$$

$$Z'_{21b} = \frac{V_2}{I_1}\bigg|_{I_2=0} = \frac{I_2 Z_{22b} + I_1 Z_{21b} + R_b(I_1+I_2)}{I_1}\bigg|_{I_2=0} = Z_{21b} + R_b \qquad (B.3)$$

$$Z'_{22b} = \frac{V_2}{I_2}\bigg|_{I_1=0} = \frac{I_2 Z_{22b} + I_1 Z_{21b} + R_b(I_1+I_2)}{I_2}\bigg|_{I_1=0} = Z_{22b} + R_b \qquad (B.4)$$

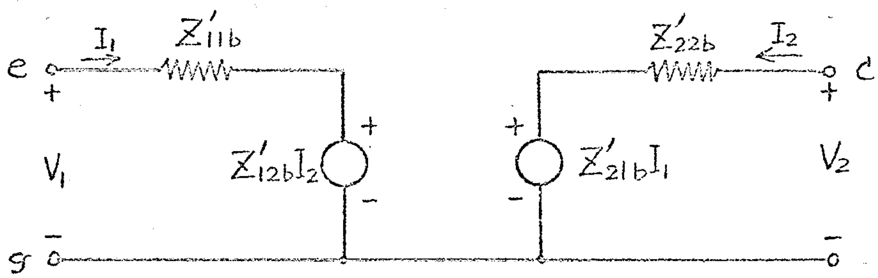

Figure B.2 Modified equivalent circuit of figure B.1

APPENDIX C

COMMON COLLECTOR Y PARAMETERS IN TERMS OF COMMON BASE Y PARAMETERS

$$Y_{11c} = Y_{11b} + Y_{12b} + Y_{21b} + Y_{22b} \quad (C.1)$$

$$Y_{12c} = -Y_{11b} - Y_{21b} \quad (C.2)$$

$$Y_{21c} = -Y_{11b} - Y_{12b} \quad (C.3)$$

$$Y_{22c} = Y_{11b} \quad (C.4)$$